Non-Markovian dynamics of a double quantum dot charge qubit with static bias

Xiufeng Cao* and Hang Zheng
Department of Physics, Shanghai Jiao Tong University, Shanghai 200240, People's Republic of China
(Received 24 January 2007; revised manuscript received 10 June 2007; published 4 September 2007)

We have studied the dynamics of charge qubit with the static bias by a perturbation treatment based on unitary transformations. The approach can be practiced for various forms of the spectral density and the usual Ohmic and piezoelectric spectra are used in our calculations. Analytical results of the quantum dynamics, described by the population inversion $P(t)$, are obtained together with the damping rate and the oscillation frequency. We find that a weak coupling of the qubit to the environment leads to a higher coherence oscillation frequency and a longer coherence time. For a fixed tunneling between the double quantum dots, the finite bias enhances the oscillation frequency effectively but its effect on the damping rate is relatively small. This is a possible way to maintain quantum coherence.

DOI: 10.1103/PhysRevB.76.115301 PACS number(s): 73.63.Kv, 73.23.Hk, 03.65.Yz, 03.67.Lx

I. INTRODUCTION

Since the quantum algorithms were proposed which can be used to solve certain computational problems much more efficiently than classical ones,[1] attention has been devoted to the physical implementation of quantum computation. Barenco *et al.*[2] discussed two possible physical realizations of the quantum controlled-NOT gate, one based on Ramsey atomic interferometry and the other on the selective driving optical resonance. Bandyopadhyay *et al.*[3] presented two different proposals for implementing mathematically reversible and dissipationless logic in nanoelectronic systems. Nanofabrication technology now allows us to design artificial atoms (quantum dots) and molecules (coupled quantum dots), in which atomic (molecular) -like electronic states can be controlled with external gate voltages.[4–6] The localized low-lying states of quantum dots (QDs) can be used to realize the reversible quantum logic gate NOT.[7] Balandin and Wang[8] proposed an implementation of the quantum controlled-NOT gate on the basis of coupled asymmetric quantum dots and Fedichkin *et al.*[9] proposed that symmetrical semiconductor quantum dots with the help of the voltage on the electrodes can carry out controlled-NOT operation. As the quantum system always interacts with its environment, quantum decoherence in the system is usually the most serious obstacle in producing efficient quantum circuits.[10–12] For this reason, a detailed understanding of quantum decoherence in open system and the possibility of implementing sufficiently large number of coherent manipulation within the characteristic coherence time of qubits are crucial for future actual implementation of quantum nanostructures for quantum information technology.

To build a quantum computer, the first step is the realization of the basic device units for quantum information processing called quantum bit (qubit), then a full set of basic logic operation. Within the last decade, various schemes have been proposed and many of them have even been realized, such as superconducting flux qubit[13–16] and solid charge qubit.[5,6,17] Among them, the gate voltage controlled semiconductor charge qubit has the potential advantages of being arbitrarily scalable to large system and compatible with the current microelectronics technology. Recently, Hayashi *et al.*[18] have successfully realized coherent manipulation of electronic state in double-dot system embedded in a GaAs/AlGaAs heterostructure containing two-dimensional electron gas. The damped oscillation of population inversion is observed in the time domain and the dependence of decoherence rate T_2^{-1} on the energy offset ε is obtained. In another similar experiment,[19] the base material used for the charge qubit is an industry-standard silicon-on-insulator wafer with a phosphorus-doped active region and all operations (initialization, manipulation, and measurement) are achieved by capacitively coupled elements. In this experiment, the static bias is controlled by the change of applied gate voltage. These experiments lead to a problem of investigation of what is the effect of the static bias on the tunneling current of the charge qubit.

Some analytical methods are used to study the dynamics of biased spin-boson model, such as the conventional perturbation theory,[20] noninteracting blip approximation,[26] Bloch-type quantum rate equation,[21] and combining (non-)Markovian master equations with correlation functions.[22] In this work, we study the coherent non-Markovian dynamics of biased spin-boson model by means of a perturbation treatment based on unitary transformations. A simple analytical expression for the population inversion or tunneling current is presented and the coherent-incoherent transition point α_c for finite bias is determined for Ohmic bath. Furthermore, decoherence induced by the piezoelectric phonons is investigated in some detail and possible means for maintaining quantum coherence are discussed.

The paper is organized as follows: In Sec. II, we introduce the model Hamiltonian for static biased spin-boson model and solve it in terms of a perturbation treatment based on unitary transformations. The results and discussions are in Sec. III. Finally, the conclusion is given in Sec. IV.

II. THEORY

The model we study is the static biased spin-boson Hamiltonian,[23]

$$H = H_s + H_b + H_i. \tag{1}$$

H_s is the Hamiltonian of the system, H_b the bosonic environment, and H_i their interaction that is responsible for decoherence.

$$H_s = -\Delta\sigma_x/2 + \varepsilon\sigma_z/2, \tag{2}$$

$$H_b = \sum_k \omega_k b_k^\dagger b_k, \tag{3}$$

$$H_i = \frac{1}{2}\sum_k g_k(b_k^\dagger + b_k)\sigma_z, \tag{4}$$

with σ_i $(i=x,y,z)$ being Pauli matrices. Δ and ε describe the tunneling coupling and the energy offset (static bias) between the two charge states, respectively. b_k^+ (b_k) and ω_k are the creation (annihilation) operators and frequency of the boson with wave vector k. In charge qubit, boson environment mainly means phonons and g_k is the electron-phonon coupling strength. In this work, we discuss the electron transport in charge qubit in zero temperature case. The effect of bath is fully described by the spectral density:

$$J(\omega) = \sum_k g_k^2 \delta(\omega - \omega_k). \tag{5}$$

In order to take into account the spin-boson correlation, we apply the following two unitary transformations. First, we make a displacement to all boson modes,

$$b_k = a_k - \frac{g_k}{2\omega_k}\sigma_0, \tag{6}$$

where σ_0 is a constant and will be determined later. Then, we apply a canonical transformation, $H' = \exp(S)H\exp(-S)$ with the generator[24,25]

$$S = \sum_k \frac{g_k\xi_k}{2\omega_k}(a_k^\dagger - a_k)(\sigma_z - \sigma_0). \tag{7}$$

ξ_k is a k-dependent function. After transformation, we decompose the transformed Hamiltonian H' into three parts,

$$H' = H_0' + H_1' + H_2', \tag{8}$$

where

$$H_0' = -\frac{1}{2}\eta\Delta\sigma_x + \frac{\varepsilon'\sigma_z}{2} + \sum_k \omega_k a_k^\dagger a_k - \sum_k \frac{g_k^2}{4\omega_k}\xi_k(2-\xi_k) + \sum_k \frac{g_k^2}{4\omega_k}\sigma_0^2(1-\xi_k)^2, \tag{9}$$

$$H_1' = \frac{1}{2}\sum_k g_k(1-\xi_k)(a_k^\dagger + a_k)(\sigma_z - \sigma_0) - i\frac{\eta\Delta}{2}\sigma_y\sum_k \frac{g_k}{\omega_k}\xi_k(a_k^\dagger - a_k), \tag{10}$$

and

$$H_2' = -\frac{\Delta\sigma_x}{2}\left\{\cosh\left[\sum_k \frac{g_k}{\omega_k}\xi_k(a_k^\dagger - a_k)\right] - \eta\right\} - i\frac{\Delta\sigma_y}{2}\left\{\sinh\left[\sum_k \frac{g_k}{\omega_k}\xi_k(a_k^\dagger - a_k)\right] - \eta\sum_k \frac{g_k}{\omega_k}\xi_k(a_k^\dagger - a_k)\right\}, \tag{11}$$

with

$$\eta = \exp\left(-\sum_k \frac{g_k^2}{2\omega_k^2}\xi_k^2\right) \tag{12}$$

and

$$\varepsilon' = \varepsilon - \tau\sigma_0, \quad \tau = \sum_k \frac{g_k^2}{\omega_k}(1-\xi_k)^2. \tag{13}$$

Obviously, H_0' can be solved exactly because the spin and bosons are decoupled. Then, we diagonalize H_0' by a unitary matrix U,

$$U = \begin{pmatrix} u & v \\ v & -u \end{pmatrix}, \tag{14}$$

with

$$u = \frac{1}{\sqrt{2}}(1-\sin\theta)^{1/2}, \quad v = \frac{1}{\sqrt{2}}(1+\sin\theta)^{1/2} \tag{15}$$

and $\sin\theta = \varepsilon'/W$ with $W = (\varepsilon'^2 + \eta^2\Delta^2)^{1/2}$. The diagonalized H' is

$$H'' = U^+ H' U = H_0'' + H_1'', \tag{16}$$

with

$$H_0'' = -\frac{1}{2}W\sigma_z + \sum_k \omega_k a_k^\dagger a_k - \sum_k \frac{g_k^2}{4\omega_k}\xi_k(2-\xi_k) + \sum_k \frac{g_k^2}{4\omega_k}\sigma_0^2(1-\xi_k)^2 \tag{17}$$

and

$$H_1'' = -\frac{1}{2}\sum_k g_k(1-\xi_k)(a_k^\dagger + a_k)\left(\frac{\varepsilon}{W}\sigma_z + \sigma_0\right) + \frac{\eta\Delta}{2W}\sigma_x\sum_k g_k(1-\xi_k)(a_k^\dagger + a_k) + i\frac{\eta\Delta}{2}\sigma_y\sum_k \frac{g_k}{\omega_k}\xi_k(a_k^\dagger - a_k).$$

σ_0 and ξ_k,

$$\sigma_0 = -\frac{\varepsilon}{W}, \quad \xi_k = \frac{\omega_k}{\omega_k + W}, \tag{18}$$

are determined in such a way that

$$H_1'' = \frac{1}{2}\varepsilon\sum_k \frac{g_k\xi_k}{\omega_k}(a_k^\dagger + a_k)(1-\sigma_z) + \frac{1}{2}\eta\Delta\sum_k \frac{g_k\xi_k}{\omega_k}[a_k^\dagger(\sigma_x + i\sigma_y) + a_k(\sigma_x - i\sigma_y)] \quad (19)$$

and $H_1''|g\rangle = 0$. This is the key point in our approach. We note that

$$\varepsilon' = \varepsilon\left(1+\frac{\tau}{W}\right), \quad \sin\theta = \frac{\varepsilon\left(1+\frac{\tau}{W}\right)}{W}. \quad (20)$$

The angle θ is in the range of $-\pi/2 \leqslant \theta \leqslant \pi/2$ and the sign of $\sin\theta$ is the same as static bias. If $\theta=0$, the model returns to zero bias case. H_2'' is of the order of $\eta g_k^2\xi_k^2/\omega_k^2$ or higher and is negligible.

We denote the ground state of H_0'' as $|g\rangle = |s_1\rangle|\{0_k\}\rangle$ and the lowest excited states as $|s_2\rangle|\{0_k\}\rangle$, $|s_1\rangle|\{1_k\}\rangle$, where $|s_1\rangle$, $|s_2\rangle$ are eigenstates of σ_z ($\sigma_z|s_1\rangle = |s_1\rangle$, $\sigma_z|s_2\rangle = -|s_2\rangle$), and $|\{n_k\}\rangle$ is the phonon state with n_k phonons for mode k. In the ground and the lowest excited states, it is easy to check that $\langle\{0_k\}|\langle s_2|H_1''|g\rangle = 0$, $\langle\{1_k\}|\langle s_1|H_1''|g\rangle = 0$, and $\langle\{0_k\}|\langle s_2|H_1''|s_1\rangle|\{1_k\}\rangle = \eta\Delta g_k\xi_k/\omega_k$. Thus, we can diagonalize H'' for these lowest-lying states through the following transformation:[24]

$$|s_2\rangle|\{0_k\}\rangle = \sum_E x(E)|E\rangle, \quad (21)$$

$$|s_1\rangle|\{1_k\}\rangle = \sum_E y_k(E)|E\rangle, \quad (22)$$

$$|E\rangle = x(E)|s_2\rangle|\{0_k\}\rangle + \sum_k y_k(E)|s_1\rangle|\{1_k\}\rangle, \quad (23)$$

where

$$x(E) = \left(1 + \sum_k \frac{V_k^2}{\left(E+\frac{1}{2}W-\omega_k\right)^2}\right)^{-1/2}, \quad (24)$$

$$y_k(E) = \frac{V_k}{E+\frac{1}{2}W-\omega_k}x(E), \quad (25)$$

with $V_k = \eta\Delta g_k\xi_k/\omega_k$. E's are the diagonalized excitation energy and are also the solutions of the equation

$$E - \frac{1}{2}W - \sum_k \frac{V_k^2}{E+\frac{1}{2}W-\omega_k} = 0. \quad (26)$$

So, the Hamiltonian can approximately be described as

$$H'' = -\frac{1}{2}W|g\rangle\langle g| + \sum_E E|E\rangle\langle E|. \quad (27)$$

The population inversion or tunneling current can be defined as $P(t) = \langle\psi(t)|\sigma_z|\psi(t)\rangle$, where $|\psi(t)\rangle$ is the total wave function in the Schrodinger picture. Since the initialization of the charge qubit is usually in the left quantum dot, it is reasonable to choose initial state $|\psi(0)\rangle = e^{-S}|L\rangle|0_k\rangle$. Then, we can obtain

$$\begin{aligned} P(t) &= \langle\psi(0)|Ue^{iH''t}U^+\sigma_z Ue^{-iH''t}U^+|\psi(0)\rangle \\ &= -u^2\sin\theta \\ &\quad - v^2\sin\theta\sum_{kk'EE'} y_{k'}^*(E')y_k(E)x(E)x^*(E)e^{i(E-E')t} \\ &\quad - v^2\sin\theta\sum_{EE'}|x(E)|^2|x(E')|^2e^{i(E-E')t} \\ &\quad + uv\cos\theta\sum_E[|x(E)|^2e^{i(E+w/2)t} + |x(E)|^2e^{-i(E+w/2)t}]. \end{aligned} \quad (28)$$

In Eq. (28), we employed the orthogonal property

$$\sum_k y_k(E)y_k(E') = \delta(E-E') - x(E)x(E'). \quad (29)$$

According to the residue theorem in complex function theory,

$$\begin{aligned} \sum_E |x(E)|^2e^{iEt} &= e^{-i(W/2)t}\frac{1}{2\pi i}\oint_C \frac{e^{i(E+W/2)t}dE}{\left(E-\frac{1}{2}W-\sum_k\frac{V_k^2}{E+\frac{1}{2}W-\omega_k}\right)} \\ &= e^{-i(W/2)t}\frac{1}{2\pi i}\oint_C \frac{e^{iE't}dE'}{\left(E'-W-\sum_k\frac{V_k^2}{E'-\omega_k}\right)}. \end{aligned} \quad (30)$$

Denoting the real and imaginary parts of $\Sigma_k \frac{V_k^2}{\omega-\omega_k\pm i0^+}$ as $R(\omega)$ and $\mp\gamma(\omega)$, respectively, we get

$$R(\omega) = \wp\sum_k \frac{V_k^2}{\omega-\omega_k} = (\eta\Delta)^2\wp\int_0^\infty d\omega' \frac{J(\omega')}{(\omega-\omega')(\omega'+W)^2},$$

$$\gamma(\omega) = \pi\sum_k V_k^2\delta(\omega-\omega_k) = \pi(\eta\Delta)^2\frac{J(\omega)}{(\omega+W)^2}, \quad (31)$$

where $\wp$ stands for Cauchy principal value and $J(\omega)$ is the spectral density. The contour integral in Eq. (30) can proceed by calculating the residue of integrand. Then, Eq. (28) reads

$$\begin{aligned} P(t) &= -\sin\theta + \sin\theta(1+\sin\theta)e^{-2\gamma(\omega_0)t} \\ &\quad + \cos^2\theta\cos(\omega_0 t)e^{-\gamma(\omega_0)t}, \end{aligned} \quad (32)$$

where ω_0 is the solution of the equation

$$\omega - W - R(\omega) = 0. \quad (33)$$

Thus, a rather simple expression for the tunneling current is obtained analytically. It should be noted here that for $t=0$, $P(t)=1$ exactly, and for $t\to\infty$, our result goes to the thermodynamical equilibrium state,[26] which is modulated by static bias

$$P(\infty) = -\sin\theta = -\frac{\varepsilon\left(1+\frac{\tau}{W}\right)}{W}. \tag{34}$$

So, our result gives not only the long time limit behavior but also the short time damping coherence oscillation, which is different from Markovian approximation. If semiconductor quantum dots are to be used as basic building blocks for quantum information processing, the coherence oscillation is very important, because the operation completely relies on it. Until now, our presentation is not restricted to any special spectral density and can be used for all kinds of baths. Finally, the electron population in the right dot and left dot can be expressed as $n_R(t)=\frac{1-\langle\sigma_z(t)\rangle}{2}=\frac{1-P(t)}{2}$ and $n_L(t)=\frac{1+\langle\sigma_z(t)\rangle}{2}=\frac{1+P(t)}{2}$.

III. RESULTS AND DISCUSSIONS

For checking our approach, Fig. 1 shows the time evolution of the electron population in the left and right dot, $n_L(t)$ and $n_R(t)$, for the ordinary Ohmic bath with finite bias, together with the result of the real-time renormalization group (RTRG) method.[27] One can see that there is a good agreement between the two results. Another check is a comparison of the long time behavior of $P(t)$ with that of the noninteracting blip approximation (NIBA).[26] Figure 2 shows the long time limit or the thermodynamic average value of the population inversion, $P(\infty)=-\varepsilon'/W$, as a function of the bias ε. Comparing with the result of NIBA, which expresses the long time limit of population inversion as $P(\infty)=-\varepsilon/\sqrt{\varepsilon^2+\Delta_r^2}$, on the scale of the figures the two curves are overlapped if the same Ohmic bath is used.

The third check is a calculation of the coherent-incoherent transition point α_c, which is defined as the point $\alpha=\alpha_c$ at which the solution of Eq. (34) is $\omega_0=0$. For $\varepsilon=0$, we have $\alpha_c=\frac{1}{2}[1+\eta\Delta/\omega_c]$, the same as what previous authors predicted.[24] For finite ε, Fig. 3 sketches the coherent-incoherent transition point α_c as a function of ε/ω_c for experimental data $\Delta=9$ μeV and $\omega_c=32.5$ μeV in Ohmic bath. One can see that α_c increases with bias significantly, which means that a moderate bias can make a wider range of the value of α for keeping the coherent oscillation. Figure 3 can be compared to the result of Monte Carlo simulations (Fig. 5 of Ref. 23) with a qualitative agreement.

Equations (31)–(34) are our main results to calculate the population inversion of charge qubit $P(t)$ as a damped coherent oscillation with frequency ω_0 and damping rate $\gamma(\omega_0)$. At zero temperature in double-dot system of GaAs material, the dominant contribution of phonons to QDs comes from the piezoelectric coupling, and the deformation coupling is small enough to be ignored. In the following, we will use the piezoelectric spectral density,[25,28]

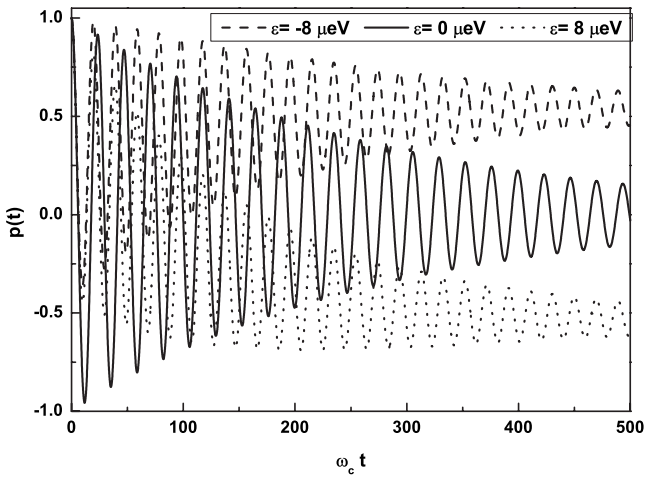

FIG. 4. The time evolution of the population difference for different values of the static bias, $\varepsilon=-8$ μeV (dashed line), 0 μeV (solid line), and 8 μeV (dotted line), in piezoelectric bath. The coupling constant is fixed as $\alpha=0.04$.

$$J(\omega) = \alpha\omega\left(1 - \frac{\omega_d}{\omega}\sin\frac{\omega}{\omega_d}\right)\theta(\omega_c - \omega), \tag{35}$$

where $\omega_c=s/l$ and $\omega_d=s/d$ (s is the sound velocity in crystal, l is the dot size, and d is the center-to-center distance between two dots) and $\theta(x)$ is the usual step function. We choose the size l as 100 nm (approximate size for the dot in Ref. 18), i.e., $\omega_c=32.5$ μeV (or 0.05 ps^{-1}). Assume the distance between two dots is sufficiently large, $d=667$ nm, correspondingly $\omega_d=0.15\omega_c$. The typical value of tunneling in experiment[18] is $\Delta=9$ μeV, which will be used throughout the paper.

The population inversion as a function of time is shown in Fig. 4 with three different static bias, $\varepsilon=-8$ μeV (dashed line), 0 μeV (solid line), and 8 μeV (dotted line), for fixed $\alpha=0.04$. The population inversion exhibits damping oscillation and the long time limit $P(\infty)$ is determined by the static bias as shown in Fig. 2. If bias is zero, $P(\infty)=0$.

The quantum coherence may be described by the oscillation frequency ω_0 and the damping rate $\gamma=T_2^{-1}$ (T_2 is the decoherence time). It has already been noticed that long coherence time is favorable for quantum manipulation. However, low oscillation frequency means that the number of quantum operation that can be achieved within the coherence time is very limited.[19] So, we must pay attention to both the damping rate and oscillation frequency. In what follows, we discuss the effect of the static bias ε, the tunneling Δ, and electron-phonon (e-p) coupling constant α on the damping rate γ and the oscillation frequency ω_0 and explain the possible means to keep the quantum coherence.

The damping rate γ versus ε relation is shown in Fig. 5(a). The e-p coupling constant $\alpha=0.02-0.07$ was used to explain the inelastic current in GaAs/AlGaAs heterostructure double QD samples[18,28] and this is the reason we show the relation with three different values of e-p coupling, $\alpha=0.04$ (solid), $\alpha=0.08$ (dashed), and $\alpha=0.12$ (dotted). The damping rate goes up with increasing bias $|\varepsilon|$ and the relationship between γ and ε agrees qualitatively with the experiment.[18] For $\varepsilon=0$ μeV and $\alpha=0.04$, the decoherence rate γ is approximately 0.02 ns^{-1}. Increasing the e-p coupling to $\alpha=0.12$, the damping rate goes up to 0.50 ns^{-1}, which is more than half of the experimental result. It proves that the coupling to piezoelectric phonons is one of the main decoherence mechanisms in this double-dot system.

The oscillation frequency ω_0 versus ε relation is shown in Fig. 5(b). The parameters are the same as those in Fig. 5(a). The oscillation frequency can be changed continually by the static bias and is a nonlinear function of ε. Setting large bias can efficiently enhance oscillation frequency. When $\alpha=0.04$ and $\varepsilon=0$ μeV, the frequency is approximately 2.1 GHz,

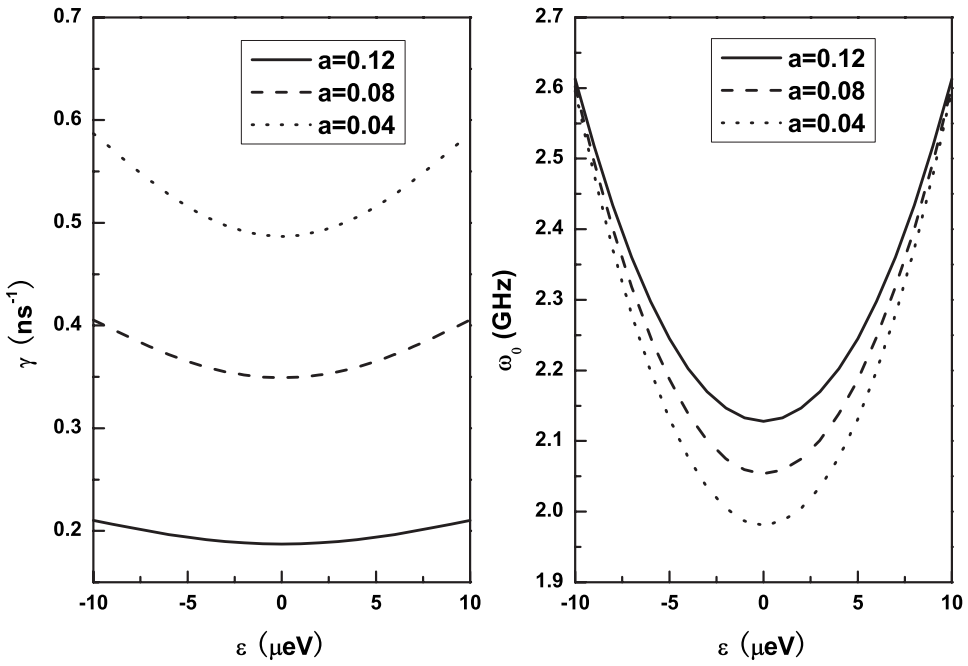

FIG. 5. (a) The damping rate γ and (b) the oscillation frequency ω_0 versus ε relations. $\Delta=9$ μeV, $\omega_d=0.15\omega_c$, and $\alpha=0.04$ (solid line), 0.08 (dashed line), and 0.12 (dotted line) in piezoelectric bath.

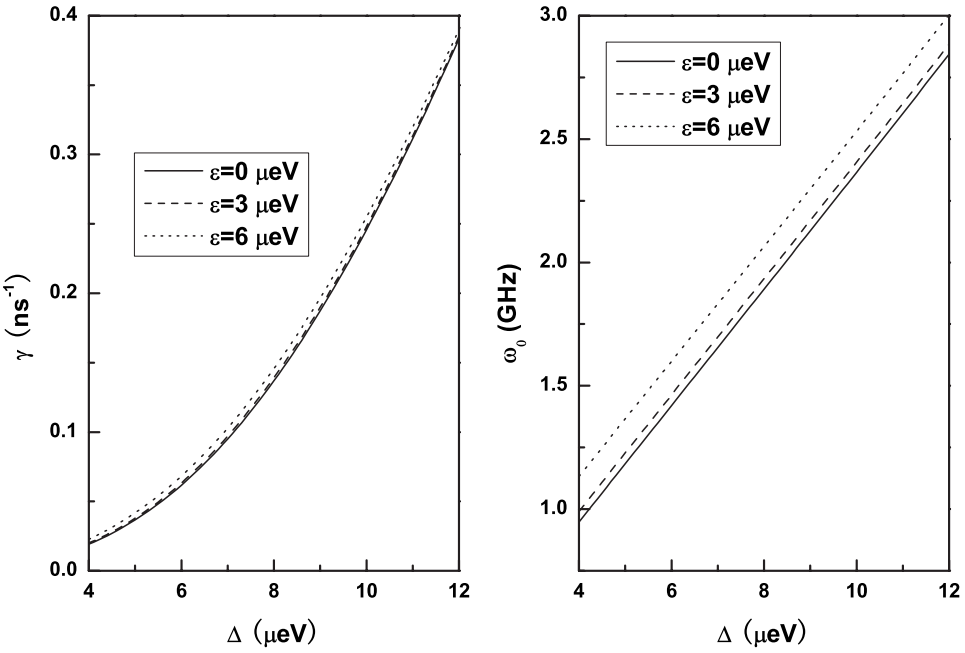

FIG. 6. (a) The damping rate γ and (b) the oscillation frequency ω versus Δ relations. $\alpha=0.04$, $\omega_d=0.15\omega_c$, and the static bias $\varepsilon=0$ μeV (solid line), 3 μeV (dashed line), and 6 μeV (dotted line) in piezoelectric bath.

which agrees well with the fitting result of the experimental data in Ref. 18. The damping rate and the oscillation frequency are symmetry functions of bias.

Figure 6(a) presents the damping rate as a function of the tunneling Δ for fixed $\alpha=0.04$ and three values of static bias, $\varepsilon=0$ μeV (solid), 3 μeV (dashed), and 6 μeV (dotted). Damping rate γ gradually increases with increasing Δ. In experiment, the tunneling Δ can be principally determined by the materials and the geometrical restriction of the dots. However, it is possible to modify the barrier tunneling by gate voltages, as was shown in Fig. 2(d) of Ref. 18. In Fig. 6(a), if Δ is of the order of several μeV, the damping rate is probably in the range of $0.2-1$ ns^{-1}, which agrees well with Ref. 18. A plot of oscillation frequency ω_0 as a function of Δ is shown in Fig. 6(b). The behavior of these curves is approximately linear. The bias effectively makes the oscillation frequency increase but its effect on the damping rate is relatively weak. Therefore, a larger static bias is a choice to preserve coherence and may be a suggestion to overcome the obstacle discussed in Ref. 19.

Our calculation indicates that for the piezoelectric coupling spectral density, the reduction of Δ makes the damping rate and the oscillation frequency decrease with almost the same order of magnitude. This may be used to explain the result of the experiment in Ref. 18, where a GaAs double quantum dot charge qubit was made with the quantum level spacing of 1.5 μeV (oscillation frequency $\omega=2.3$ GHz). For the silicon two-level quantum system in Ref. 19, the characterized energies $E^*=40.5$ neV correspond to angular frequency $\omega=62$ MHz, which is 1/37 smaller than that of Ref. 18. However, the coherence time of the silicon QD is 2 orders longer than that reported for GaAs QD. The lack of piezoelectric coupling in silicon might be the main reason for the difference behavior between the silicon QD and the GaAs QD.

Figure 7 presents the damping rate γ and oscillation frequency ω_0 as functions of the coupling α for different values of the bias, $\varepsilon=0$ μeV (solid), 3 μeV (dashed), and 6 μeV (dotted). For fixed bias, the damping rate γ increases but the oscillation frequency decreases with increasing α. As a result, to keep the coherence of charge qubit for a long time, one should diminish the coupling but ensure the effective interdot coupling and static bias, either by finding good material with small e-p coupling, by modifying the design of the double QD structure, or by better gate tuning.

IV. CONCLUSION

We have studied the dynamics of charge qubit with the static bias by a perturbation treatment based on unitary transformations. The approach is fit for various forms of the spectral density and the usual Ohmic and piezoelectric spectra are used in our calculations. Analytical results of the quantum dynamics, described by the population inversion $P(t)$, are obtained together with the damping rate and the oscillation frequency. We find that a weak coupling of the qubit to the environment leads to a higher coherence oscillation frequency and a longer coherence time. For a fixed tunneling between the double quantum dots, the finite bias enhances the oscillation frequency effectively but its effect on the damping rate is relatively small. This is a possible way of maintaining quantum coherence. Besides, our approach is quite simple, but its output is in good agreement with those of previous authors using various complicated methods.

The purpose of our unitary transformation is to find a better way of dividing the transformed Hamiltonian into unperturbed part H_0'', which can be treated exactly, and $H_1''+H_2''$, which may be treated by perturbation theory. By choosing the form of η [Eq. (12)], ξ_k, and σ_0 [Eq. (18)], it is possible to treat H_1'' and H_2'' as perturbation because of the following reasons: (1) If we treat the coupling term in the

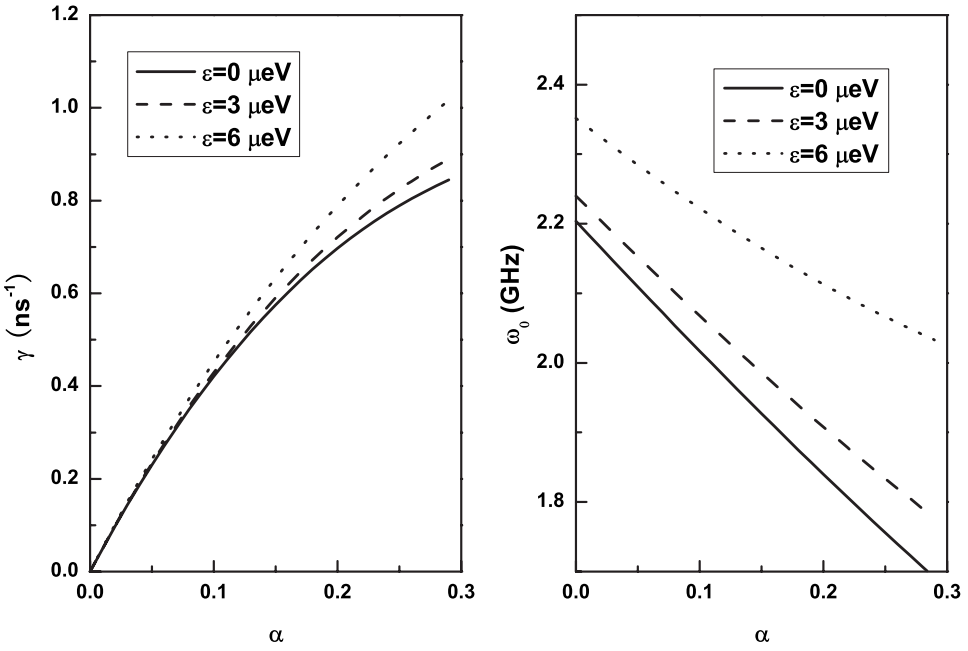

FIG. 7. (a) The damping rate γ and (b) the oscillation frequency ω versus α relations. $\Delta=9$ μeV, $\omega_d=0.15\omega_c$, and the static bias $\varepsilon=0$ μeV (solid line), 3 μeV (dashed line), and 6 μeV (dotted line) in piezoelectric bath.

original Hamiltonian H as the perturbation, the dimensionless expanding parameter is $\Sigma_k g_k^2/\omega_k^2$. For Ohmic bath ($s=1$), it is $2\alpha\int d\omega/\omega$, which is logarithmically divergent in the infrared limit, but for the coupling in transformed Hamiltonian H'', the expanding parameter is $\Sigma_k g_k^2\xi_k^2/\omega_k^2 \sim 2\alpha\int d\omega\omega/(\omega+\eta\Delta)^2$, which is finite in the infrared limit. (2) H_1'' can be treated as perturbation because it satisfied $H_1''|g\rangle=0$. It is shown that the ground state energy correction of H_1'' is zero. H_2'' may be omitted because its contribution is zero at second order of g_k.

ACKNOWLEDGMENTS

This work was supported by the National Natural Science Foundation of China (Grants No. 10474062 and No. 90503007).

*cxf@sjtu.edu.cn

[1] M. A. Nielsen and I. L. Chuang, *Quantum Computation and Quantum Information* (Cambridge University Press, Cambridge, 2000).
[2] A. Barenco, D. Deutsch, A. Ekert, and R. Jozsa, Phys. Rev. Lett. **74**, 4083 (1995).
[3] S. Bandyopadhyay, A. Balandin, V. P. Roychowdhury, and F. Vatan, Superlattices Microstruct. **23**, 445 (1998).
[4] S. Tarucha, D. G. Austing, T. Honda, R. J. van der Hage, and L. P. Kouwenhoven, Phys. Rev. Lett. **77**, 3613 (1996).
[5] T. H. Oosterkamp, T. Fujisawa, W. G. van der Wiel, K. Ishibashi, R. V. Hijman, S. Tarucha, and L. P. Kouwenhoven, Nature (London) **395**, 873 (1998).
[6] Toshimasa Fujisawa, Tjerk H. Oosterkamp, Wilfred G. van der Wiel, Benno W. Broer, Ramón Aguado, Seigo Tarucha, and Leo P. Kouwenhoven, Science **282**, 932 (2001).
[7] L. A. Openov, Phys. Rev. B **60**, 8798 (1999).
[8] A. Balandin and K. L. Wang, Superlattices Microstruct. **25**, 509 (1999).
[9] L. Fedichkin, M. Yanchenko, and K. A. Valiev, Nanotechnology **11**, 387 (2000).
[10] V. N. Stavrou and Xuedong Hu, Phys. Rev. B **72**, 075362 (2005).
[11] W. G. Unruh, Phys. Rev. A **51**, 992 (1995).
[12] S. D. Barrett and G. J. Milburn, Phys. Rev. B **68**, 155307 (2003).
[13] P. Bertet, I. Chiorescu, G. Burkard, K. Semba, C. J. P. M. Harmans, D. P. DiVincenzo, and J. E. Mooij, Phys. Rev. Lett. **95**, 257002 (2005).
[14] I. Chiorescu, P. Bertet, K. Semba, Y. Nakamura, C. J. P. M. Harmans, and J. E. Mooij, Nature (London) **431**, 159 (2004).
[15] I. Chiorescu, Y. Nakamura, C. J. P. M. Harmans, and J. E. Mooij, Science **299**, 1869 (2003).
[16] A. Lupascu, E. F. C. Driessen, L. Roschier, C. J. P. M. Harmans, and J. E. Mooij, Phys. Rev. Lett. **96**, 127003 (2006).
[17] S. Gardelis, C. G. Smith, J. Cooper, D. A. Ritchie, E. H. Linfield, Y. Jin, and M. Pepper, Phys. Rev. B **67**, 073302 (2003).
[18] T. Hayashi, T. Fujisawa, H. D. Cheong, Y. H. Jeong, and Y. Hirayama, Phys. Rev. Lett. **91**, 226804 (2003).
[19] J. Gorman, D. G. Hasko, and D. A. Williams, Phys. Rev. Lett. **95**, 090502 (2005).
[20] L. Fedichkin and A. Fedorov, Phys. Rev. A **69**, 032311 (2004).
[21] S. A. Gurvitz, L. Fedichkin, D. Mozyrsky, and G. P. Berman, Phys. Rev. Lett. **91**, 066801 (2003).
[22] Ramon Aguado and Tobias Brandes, Phys. Rev. Lett. **92**, 206601 (2004).

[23] Klaus Volker, Phys. Rev. B **58**, 1862 (1998).
[24] H. Zheng, Eur. Phys. J. B **38**, 559 (2004).
[25] Z. J. Wu, K. D. Zhu, X. Z. Yuan, Y. W. Jiang, and H. Zheng, Phys. Rev. B **71**, 205323 (2005).
[26] A. J. Leggett, S. Chakravarty, A. T. Dorsey, M. P. A. Fisher, A. Garg, and W. Zwerger, Rev. Mod. Phys. **59**, 1 (1987); U. Weiss, *Quantum Dissipative System* (World Scientific, Singapore, 1993).
[27] Markus Keil and Herbert Schoeller, Phys. Rev. B **63**, 180302(R) (2001).
[28] T. Brandes and T. Vorrath, Phys. Rev. B **66**, 075341 (2002).